JOURNAL OF SPACECRAFT AND ROCKETS
Vol. 43, No. 2, March–April 2006

Arcjet Screening of Candidate Ablative Thermal Protection Materials for Mars Science Laboratory

Bernard Laub* and Susan White†
NASA Ames Research Center, Moffett Field, California 94035

Arc plasma tests of a range of ablative materials considered candidates for the thermal protection system for the Mars Science Laboratory are described. The objective of these tests was to identify ablative thermal protection materials that offer weight, performance, cost, or other advantages relative to SLA-561V. Several low-density silicones with a mixture of low-density fillers and polymer-impregnated ceramics were tested in the Ames Interaction Heating Facility at conditions representative of nominal stagnation point and worst-case conical heating on the Mars Smart Lander forebody. A wide variety of low-density ablatives and impregnated flexible materials were tested in the Ames Panel Test Facility at nominal and worst-case heating for the Mars Smart Lander backshell. The results of these tests have identified several attractive materials worthy of further investigation.

Introduction

THE objective of the Mars Science Laboratory (MSL) project is precision landing of a large science payload on the surface of Mars to support further robotic exploration of the planet's surface prior to an attempt to return Martian material to Earth (i.e., Mars sample return mission).

Aerothermal Environment

A conservative, preliminary estimate of peak heating rates and heat loads was provided by NASA Langley Research Center (LaRC) based on Monte Carlo analyses of 2005 entry trajectories employing the Program to Optimize Simulated Trajectories (POST).[1] For these analyses, LaRC assumed a baseline shape with a 0.9124 nose radius, a 3.75-m-diam aeroshell, an entry mass of 1950 kg, and a trim angle of attack of 16 deg. The POST solution for the stagnation point heating rate and heat load for the maximum heat flux trajectory is shown in Fig. 1.

Computational fluid dynamics (CFD) solutions generated by LaRC using the Langley Aerothermodynamic Upwind Relaxation Algorithm (LAURA)[2–4] indicate a high probability of boundary-layer transition on the forebody at a location between 35–44% of the distance between the nose and the shoulder just prior to the time of peak heating. LaRC estimated peak heating rates at various locations on the MSL shape based on a combination of the POST stagnation-point solutions, LAURA CFD solutions, heating augmentation caused by a turbulent boundary layer, and applied safety margins to compensate for uncertainties in the fidelity of aerodynamic heating predictions. The peak heating rates are shown in Fig. 2.

The values shown in Fig. 2 were generated with assumptions of a supercatalytic, radiative equilibrium surface boundary condition and encompass the range from nominal to worst case where the worst-case values include margins caused by uncertainties. The uncertainties are dependent on the confidence with which aerodynamic heating can be predicted and varies along the body. For example, LaRC assigned a safety margin of ≈25% at the stagnation point, but a margin of 300% is included on the afterbody. It is anticipated that as the project proceeds and more experimental data and CFD solutions are developed the uncertainties in heating and the associated margins will be reduced.

Reference Thermal Protection System Sizing

With concurrence from the Jet Propulsion Laboratory (JPL), SLA-561V was selected as the reference thermal protection system (TPS) for initial MSL studies. SLA-561V is a low-density silica fiber, silicone and cork composite, hereinafter "cork silicone," in a Flexcore™ honeycomb, developed and manufactured by Lockheed Martin Astronautics, with a flight heritage extending back to the middle 1970s on the Mars Viking probes. It has subsequently been used as the forebody TPS on Mars Pathfinder (MPF) and is currently being designed as the forebody TPS on the Mars Exploration Rover (MER) scheduled for launch in 2003. SLA-561S is a sprayable version of the cork silicone that was developed as insulation for the shuttle external tank and was used successfully as the backshell TPS on MPF and will be used in a similar application for MER.

NASA Ames Research Center (ARC) used existing numerical models for SLA-561V to estimate thickness requirements for the stagnation-point heating shown in Fig. 2. The requirement was to maintain the bondline between the TPS and the underlying aluminum honeycomb substructure below the maximum allowable adhesive temperature of 250°C. Scaling factors were applied to the stagnation-point heating to determine the sensitivity of TPS thickness to heating. The results are shown in Fig. 3.

The highest peak heating rates shown in Fig. 2 (without consideration of the shoulders or corners) are 140 W/cm^2 on the forebody and 17 W/cm^2 on the backshell (an average between the corner and the cone). Utilizing the appropriate scale factor from Fig. 3, a uniform forebody TPS thickness of 14 mm of SLA-561V was defined, corresponding to an areal weight (areal weight = density × thickness) of 0.36 g/cm^2. A similar approach on the backshell resulted in a uniform TPS thickness of 7.4 mm of SLA-561V with a corresponding areal weight of 0.19 g/cm^2.

Candidate Forebody TPS Materials

The criteria for selecting candidate ablative materials for the MSL forebody TPS were defined by NASA ARC in consultation with JPL. The primary criteria were that the materials already exist, the virgin density ≤ virgin density of SLA-561V, and a modest surface recession is anticipated at the highest heat flux (140 W/cm^2).

A list of candidate materials satisfying these criteria was assembled by NASA ARC TPS experts and reviewed with JPL, NASA Johnson Space Center (JSC), and NASA LaRC. By mutual agreement, an initial list of candidate forebody ablative TPS

Presented as Paper 2002-4507 at the AIAA Atmospheric Flight Mechanics Conference, Monterey, CA, 5–8 August 2002; received 3 January 2003; revision received 1 August 2004; accepted for publication 1 February 2005.

*Project Manager, MS 234-1, Thermal Protection Materials and Systems Branch. Associate Fellow AIAA.
†Senior Researcher, MS 234-1, Thermal Protection Materials and Systems Branch.

Table 1 Candidate ablative materials for MSL forebody TPS

Candidate materials	Density, lbm/ft^3	Density, kg/m^3	Comments
SLA-561V (Lockheed Martin Astronautics)	16	256	Current low-density reference material with flight heritage (not tested here)
Hyperlite A: Fully dense (FD) and reduced density (RD) (Applied Research Associates)	12.5–13.2	200–212	Low-density silicone composite with a mixture of low-density fillers; some arcjet test data exist.
Hyperlite B	12	192	Low-density silicone composite with a mixture of low-density fillers; some arcjet test data exist.
SRAM	14–17	224–272	Alternate low-density silicone composite with a mixture of low-density fillers; some arcjet test data exist.
NASA SIRCA-15F	15	240	Silicone-impregnated ceramic; thermal performance similar to SLA; flight qualified for certain uses
NASA Advanced SIRCA (new)	16	256	New development with improved method of impregnating silicone into ceramic; char yield (of silicone) can be tailored.
NASA Blacktile: silicone-impregnated refractory tile (new)	16	256	New ARC development of low-density toughened tile
NASA TUFROC (new)	Variable	Variable	New ARC development of high-temperature ceramic tile with low-catalycity, high-emissivity ceramic coating; some arcjet test data exist (not tested).

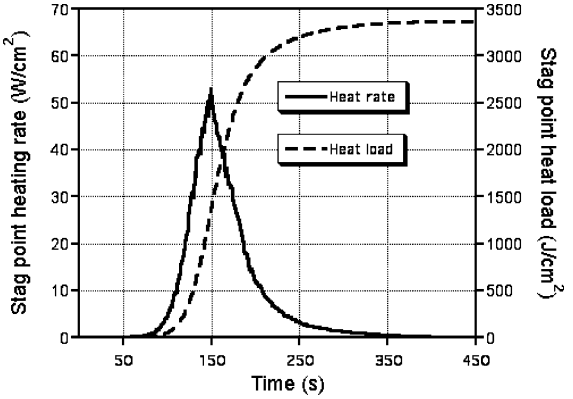

Fig. 1 POST solutions for stagnation-point heating on max heat-flux trajectory.

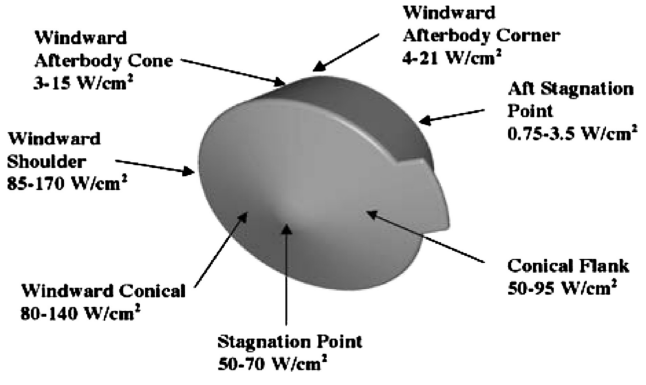

Fig. 2 Maximum heating rates on MSL.

materials was selected for comparative arcjet screening as shown in Table 1.

The selection of SLA-561V was obvious as it was chosen as the reference material for the preliminary design of the MSL forebody TPS. Unfortunately, SLA-561V was not tested in the forebody screening series because samples could not be procured in time from Lockheed Martin because of project constraints. However, SLA-561S was provided by Lockheed Martin, and was tested at the backshell heating conditions.

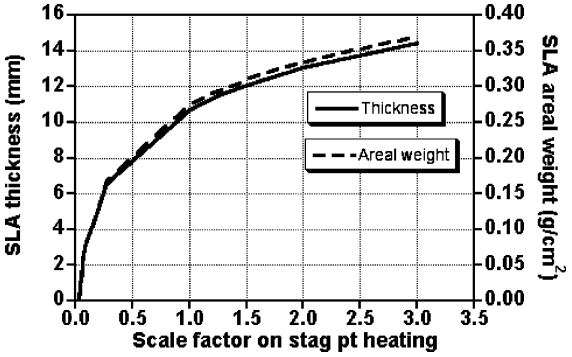

Fig. 3 Variation of SLA thickness and areal weight with heating.

Applied Research Associates, Inc. (ARA) has been developing a family of low-density silicone and phenolic-based materials[5,6] with densities in the range from 176 to 448 kg/m^3. Many of these materials have been tested in arcjet facilities at NASA under Small Business Innovative Research (SBIR) programs sponsored by ARC and JSC.

Silicone-impregnated reusable ceramic ablator (SIRCA[7]) is a NASA ARC-invented material that has been successfully employed as the back interface plate on MPF and was employed in a similar application and as nozzle covers on MER.

Advanced SIRCA is a NASA ARC development wherein the technique for impregnating the ceramic tile with silicone has been modified to improve fabrication. An advantage of this modified technique is that the composition of the silicone impregnant can be altered to tailor the char yield of the silicone.

Blacktile[8] is a recent NASA ARC development wherein a silicon oxycarbide (SiOC) tile is created and then impregnated with a silicone compound. The resultant material is a black (i.e., high emittance) ceramic with the potential for higher temperature performance.

Toughened unipiece fibrous refractory oxidation-resistant ceramic (TUFROC) is a new NASA ARC development that employs an oxidation-resistant low-density carbon fiberform backed by a low-density ceramic insulator, all encased in a new, low-catalycity ceramic coating that is capable of significantly higher surface temperatures than current ceramic coatings. As a multilayered material, the density is dependent on the thickness of each layer. Unfortunately, TUFROC was not tested in this screening series because it could not be fabricated to satisfy the areal weight requirement,

because there is a minimum thickness requirement for the outer carbon insulator layer.

Arcjet Screening Tests of Candidate Forebody TPS Materials

A series of screening tests was conducted in the NASA ARC 60-MW Interaction Heating Facility (IHF) wherein samples of all ablative forebody TPS candidate materials were evaluated with square heat pulses at two test conditions: 1) the nominal stagnation-point peak heat flux, that is, 50 W/cm^2 (hot wall), and 2) the highest peak heat flux (with margins) on the conical flank, that is, 140 W/cm^2 (hot wall).

All tests were conducted in air as the capability to test in a simulated Mars atmosphere (primarily CO_2) does not exist in IHF at this time. All samples were 10.16-cm-diam, flat-faced cylinder stagnation models with a corner radius of 0.95 cm. Calorimeter and Teflon® models with the same geometry were used to establish and verify heat flux[9] and heating uniformity. The thicknesses of the samples for each material were tailored to attempt to achieve an ideal areal weight of 0.36 g/cm^2, which corresponds to the predicted areal weight of SLA-561V required to limit the bondline temperature to 250°C for worst-case heating. Consequently, samples of the lower-density materials were thicker than samples of the higher-density materials.

As common practice, screening tests have usually been conducted on materials of equal thickness, but, given the variations in density among candidate materials, the resultant data from such tests would not provide a simple means of evaluating comparative performance between the candidates. Because minimum TPS weight is a goal of MSL, conducting tests at equal areal weight allows a direct and meaningful comparison of maximum bondline temperature. The tests at the nominal stagnation-point heating rate, where little surface recession would be expected, allows a direct comparison of insulation performance. The lowest-density materials would be expected to have an advantage at this condition. However, by also testing at a more severe condition where surface recession is anticipated, it would be expected that the higher-density materials would exhibit comparatively more resistance to recession. The "best" materials would be those with the lowest maximum bondline temperatures at both conditions and "acceptable" surface recession at the high heat-flux condition.

Each sample was bonded with RTV-560 to a substrate that consisted of 0.5-mm-thick aluminum facesheets on 6.35-mm-thick aluminum honeycomb. All samples had two centered Type-K thermocouples in the adhesive bond, and surface temperature was monitored with a two-color pyrometer. All tests were run for 68 s, and thermocouple data were recorded after the samples were removed from the flow to record peak bondline temperature during thermal soak. Posttest evaluation included measurements of mass loss, surface recession, and char depth as well as an assessment of relevant surface features. In general, two samples of each material were tested at each condition.

Figure 4 illustrates the surface recession for each material at each of the two test conditions. The Teflon® samples were run for sufficient duration to ideally cause 2.5-mm recession. As seen at the low heat-flux condition, the surface recession, if any, was minimal. However, at the high heat-flux condition the data demonstrated a significant range of surface recession among the candidate materials.

For example, ARA's Hyperlite A/RD receded about 10 mm at the high heat-flux condition. Furthermore, there was more recession near the edge of the sample than in the middle, although the edges of all of the worst-case heat-flux models had been sealed to limit edge porosity and radial flow-through. At higher heat fluxes, a SIRCA collar could have been used for this purpose, but that was not considered necessary at these test conditions. Because Teflon® control samples were also tested and demonstrated heating uniformity, and the other materials tested in this series did not exhibit enhanced recession near the edge, it was concluded that near the edge of the lowest-density ARA samples, the pyrolysis products were venting out the side rather than the front. This side venting eliminated the heating reduction in that region that mass injection usually provides.

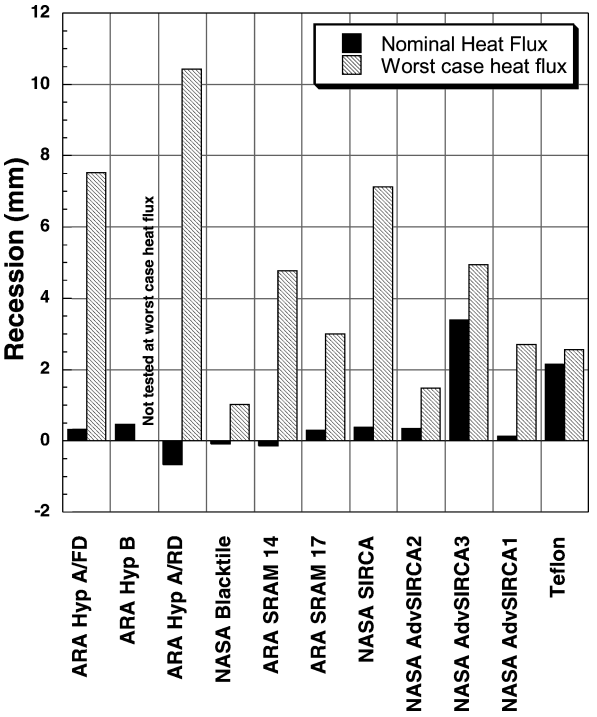

Fig. 4 Surface recession of candidate forebody TPS materials.

Consequently, ARA introduced samples of a material (SRAM 14) with similar composition but higher density, which, as seen in Fig. 4, experienced about half the recession of Hyperlite A/RD at the high heat-flux condition and uniform recession across the sample face. The SRAM-17 recessions given are corrected because the original measurement methods used for the other samples yielded ambiguous results for SRAM-17.

Another interesting result was the recession of SIRCA in comparison to advanced SIRCA. Three versions of advanced SIRCA were tested with the composition of the silicone impregnant tailored to provide three different char yields. These silica-based ceramic materials melted and flowed at the high heat-flux condition, whereas there was no evidence of melting at the lower heat-flux condition. At the low heat flux, char formation turned SIRCA from white to black as expected. As seen in Fig. 4, advanced SIRCA(1) reduced the recession by almost a factor of three in comparison to SIRCA, which experienced almost 7.6 mm (0.3 in.) of recession at the high heat-flux condition. Advanced SIRCA(2) experienced surface recession about half of that of advanced SIRCA(1). Clearly, these tests demonstrated that tailoring the composition and resultant char yield of the silicone impregnant could have a significant effect on material surface response. Of some interest was the performance of Blacktile. As seen in Fig. 4, it experienced the smallest surface recession at the high heat flux from among all of the candidate ablative materials. Given that the density of the substrate and impregnant was similar to the other ceramic SIRCA materials, this result was intriguing as there was no evidence of melt.

Figure 5 shows a pretest photo of ARA's SRAM 14 on the left and posttest photos for nominal heating (middle) and worst-case heating (right). It is interesting to note how the material is fabricated, that is, in ribbons that are bonded together with a glass fabric at the interface. Unlike SLA-561V, which uses a phenolic fiberglass honeycomb reinforcement, this fabrication technique is simpler and, potentially, less costly. Although the glass interface ribbons are apparent, the surface is typical of a charring ablator with no evidence of melt. The posttest photo of SRAM 14 after worst-case heating shows the expected charring and a smooth but receded surface.

Figure 6 includes pre- and posttest photos of SIRCA. As seen, the pretest material is white and after testing at the low heat flux exhibits a black, charred surface from the expected conversion of silicone. However, the posttest photo from the high heat-flux test exhibits a glassy surface that has melted and flowed.

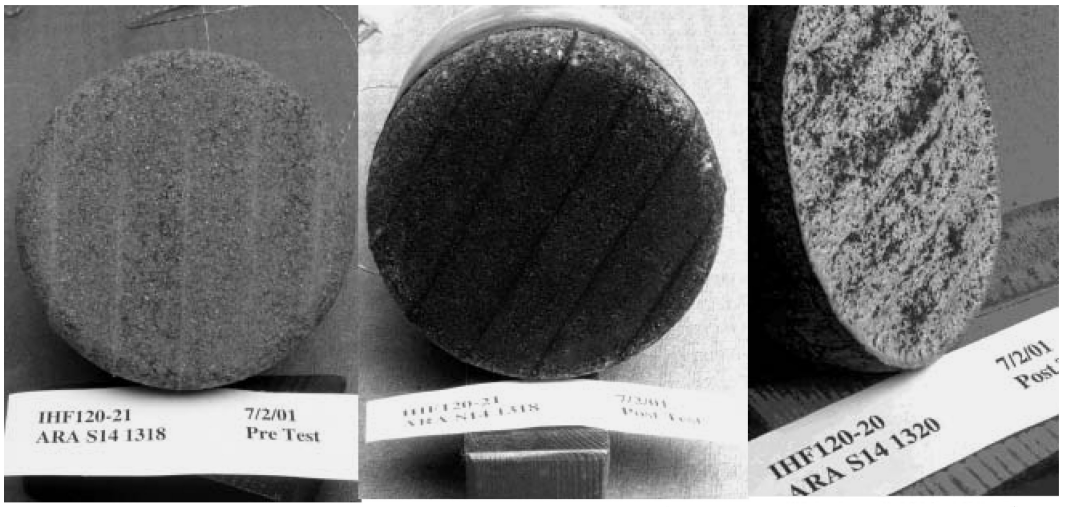

Pretes Posttest at 50 W/cm^2 Postest at 140 W/cm^2

Fig. 5 Pre- and posttest photos of ARA cork silicone materials.

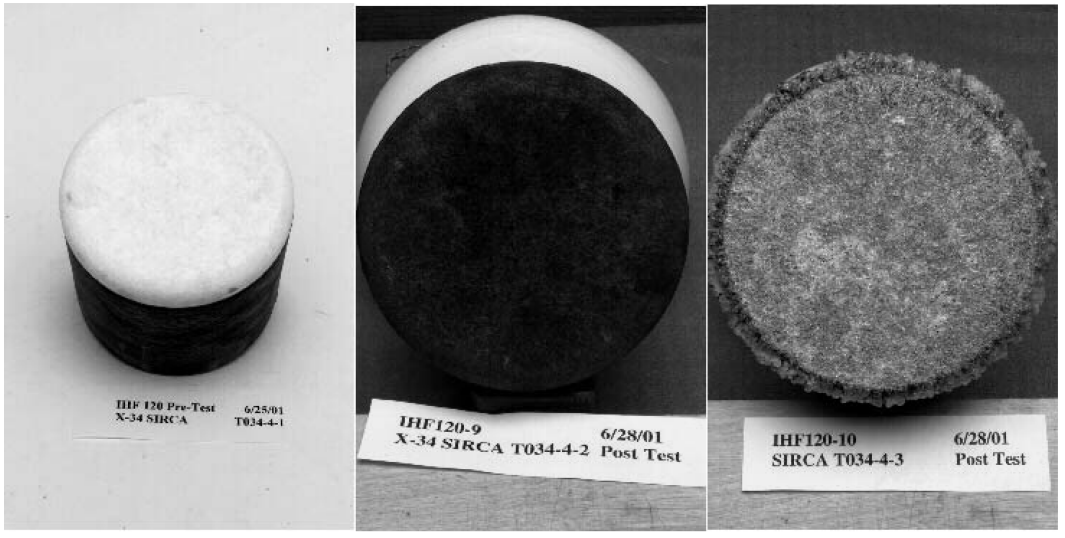

Pretest Posttest at 50 W/cm^2 Posttest at 14 Postest

Fig. 6 Pre- and posttest photos of SIRCA.

Figure 7 illustrates the peak bondline temperatures attained by the candidate materials at each of the two test conditions. As seen, the ARA silicone-based ablators exhibit significantly lower bondline temperatures than any of the ceramic materials, at both the high and low heat-flux conditions. The relatively limited range of temperatures for the ceramic-tile-based materials at the lower heat flux is a reasonable indication that the insulation capability of these materials is quite similar. The results at the higher heat flux suggest that the ablation process experienced by the ceramic materials removes enough energy to compensate for the decreasing thickness. This effect is best illustrated by comparing the peak bondline temperatures for Blacktile, which had the lowest recession among these materials, with the peak bondline temperature for SIRCA, which had the greatest recession. This tradeoff between bondline temperature and recession is the classic result of ablation sacrificing mass to control temperature.

Candidate Backshell TPS Materials

The criteria for selecting candidate ablative materials for the MSL backshell TPS were defined in consultation with JPL. The selection criteria were not as stringent on the backshell as for the forebody because the backshell for MSL, as currently conceived, is not load carrying and no equipment is attached (either externally or internally). In fact, the backshell is removed at deployment of the supersonic parachute. The objective of the backshell TPS is to efficiently handle the entry heat load at minimal weight. Because a substructure might not be required, flexible materials were considered in addition to classical rigid materials. A list of candidate materials was assembled by NASA ARC and reviewed with TPS experts from JPL, NASA JSC, and NASA LaRC. By mutual agreement, an initial list of candidate backshell ablative TPS materials was selected for comparative arcjet screening as shown in Table 2.

Arcjet Screening Tests of Candidate Backshell TPS Materials

A series of screening tests was conducted in the NASA ARC 20 MW Panel Test Facility (PTF) wherein samples of all ablative backshell TPS candidate materials were evaluated at two test conditions: 1) an average nominal backshell peak heat flux, that is, 5 W/cm^2 (hot wall), and 2) an average worst-case peak heat flux on the windward afterbody, that is, 17 W/cm^2 (hot wall), value between corner and cone.

These wedge test samples were either square or rectangular, dependent on the ability to acquire and/or fabricate samples in the available time. The preferred sample was a 10.16×20.32 cm rectangle. The thickness of the samples for each material was tailored to achieve a uniform areal weight of 0.19 g/cm^2, which corresponds to the predicted areal weight of SLA-561V required to limit the

Table 2 Candidate ablative materials for MSL backshell TPS

Candidate materials	Density, lbm/ft^3	Density, kg/m^3	Comments
SLA-561S (sprayable)	16	256	Current low-density std with flight heritage
Hyperlite silicones with a mixture of low density fillers	11–13	176–208	Low-density silicone foams; some arc test data
FIREX RX2390 intumescent foam (Pfizer)	78	1250	Tested at 5–11 W/cm^2 (evaluated for tactical missile TPS applications)
Boeing P45 cork	21	336	MMIII booster and shroud TPS; simple and inexpensive application
Acusil-II	16	256	RF transparent material currently used over TMD target antennas: simple fabrication
NASA flexible ablator aerogel composite	12–16	192–256	New ARC development to create a candidate flexible low-density ablator

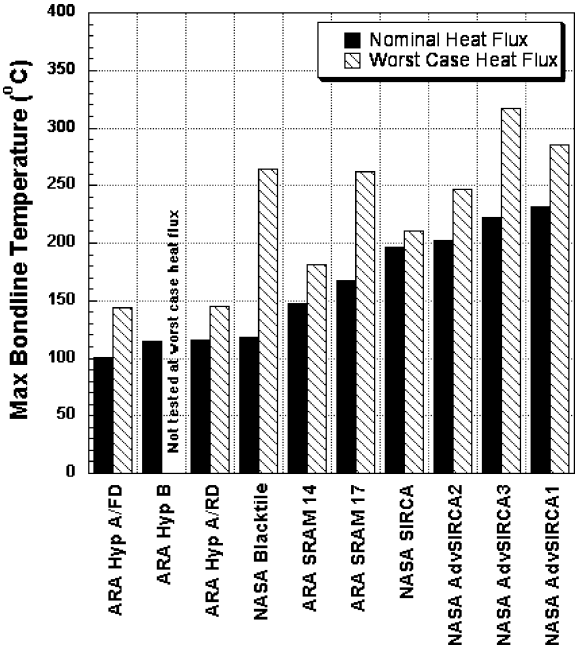

Fig. 7 Maximum bondline temperature of candidate forebody TPS materials.

bondline temperature to 250°C for worst-case heating. Each sample was bonded with RTV-560 to a substrate that consisted of 0.5-mm-thick aluminum facesheets on 6.35-mm-thick aluminum honeycomb. All samples had centered type K thermocouples in the adhesive bond, and surface temperature was monitored with an optical pyrometer. All tests were run for 68 s, and thermocouple data were recorded after the samples were removed from the flow to record peak bondline temperature during thermal soak. Posttest evaluation included measurements of mass loss, surface recession, and char depth as well as an assessment of relevant surface features. In general, two samples of each material were tested at each condition.

The PTF provides a supersonic tangential flow over a flat 50×50 cm test box that contains the test articles. Normally, the front-central region is utilized for the test articles. That was the case here as well. Typical operation of the PTF does not allow the test articles to be totally isolated from the flow during facility startup. The test box is maintained at a small negative angle of attack (relative to the flow) during facility startup and stabilization. Then the test box is brought into the flow at a zero or small positive angle of attack to attain the desired test condition on the test articles. However, this

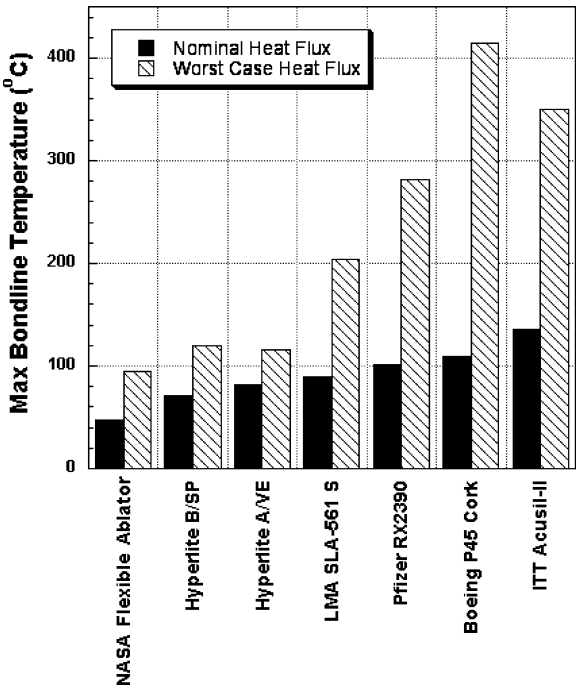

Fig. 8 Maximum bondline temperature of candidate backshell TPS materials.

procedure does allow the test articles to experience some preheating prior to insertion into the flow.

Figure 8 illustrates the maximum bondline temperatures exhibited by the candidate backshell TPS materials at both heating conditions. As seen, at the lower heat flux all materials had maximum bondline temperatures well below the 250°C criterion, as expected. However, the NASA flexible aerogel composite and both of ARA's low-density silicone-based ablators exhibited slightly lower bondline temperatures than the SLA-561S. This trend was also evident at the higher heat flux and, for the NASA flexible aerogel composite, and the ARA low-density silicones, the differences relative to SLA-561S are more significant.

At the higher heat-flux condition the SLA-561S samples exhibited significant char spallation. The P-45 cork samples (which Boeing supplied with a coating) developed "blisters" at the higher heat-flux condition. The RX2390 intumescent exhibited very modest char swell and was a rugged material (which was not surprising given its virgin density). Acusil II did not exhibit any anomalous behavior at either heating condition but just is not as good an insulator as the other candidate materials.

Figure 9 illustrates a comparison of the surface recession exhibited by the candidate backshell materials at the two test conditions. The materials are listed in the same order as in Fig. 8. As seen, the NASA flexible aerogel composite exhibited fairly small surface recession. In itself, this minimal surface recession is not a discriminator because the Acusil II also exhibited very small recession, but its maximum bondline temperatures were among the highest. The ARA low-density silicones exhibited very modest recession at the lower heat flux but more substantial recession at the higher heat flux. In general. the lower-density materials experienced more recession than the higher-density versions. The relatively large recession exhibited by the SLA-561S at the higher heat flux reflects the effects of char spallation.

Figure 10 shows pretest (Fig. 10a) and posttest (Fig. 10b and 10c) photos of the ARA low-density silicone materials. In each photo, the material in the top half with reinforcing fabric ribbons normal to the flow is called Hyperlite A/VE. The material in the bottom half of the photo is called Hyperlite B/SP. The posttest photo from the test at 5 W/cm^2 (Fig. 10b) exhibits very little change in color or dimensions. The posttest photo at the higher 17 W/cm^2 condition (Fig. 10c) exhibits more significant color change, typical of charring

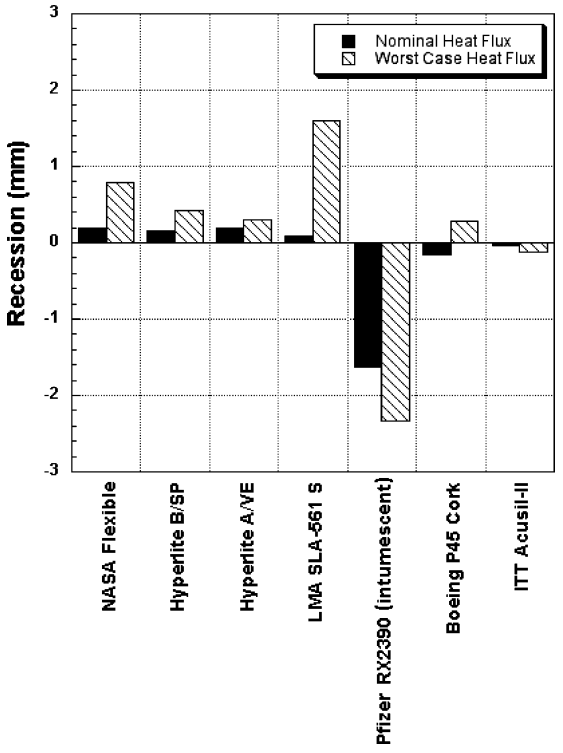

Fig. 9 Surface recession of candidate backshell TPS materials.

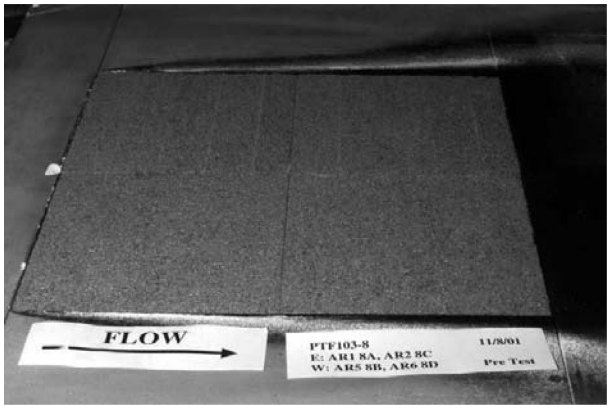

Fig. 10a Pretest photo of ARA Hyperlite silicones with a mixture of low-density fillers.

ablators, and surface cracking (appearance similar to a dried mud flat), which is very typical of cork-based materials. Hyperlite A/VE exhibited apparent separation from the reinforcing ribbons. It is believed to be caused by faster ablation of the reinforcing strip-to-strip bonding adhesive compared to the rest of the material. The surface cracking seen in Hyperlite B/SP is a cooldown phenomenon and does not influence material performance in a single use application. The thermal performance of Hyperlite was very good, providing the second-best bondline temperatures of all screened materials.

Figure 11 shows pretest and posttest photos of the NASA flexible aerogel composite materials. The pretest setup is shown in Fig. 11a showing sample sizes of 5-in. (10.16 cm) square, which appear different in color. Two samples had a whitish look while the other two had a brown-blue appearance. This difference is indicative of different aerogel infiltrants. Figure 11b shows the posttest appearance after the test at 5 W/cm^2. It is seen that the whitish samples turned light blue, and the blue-brown samples turned a deeper blue. Further color change is evident in the posttest photo from the 17-W/cm^2 test, but there is no evidence of surface recession or other surface anomalies. In this test layout, white ceramic fibers were stuffed into gaps between the worst-case test samples, and around the outer

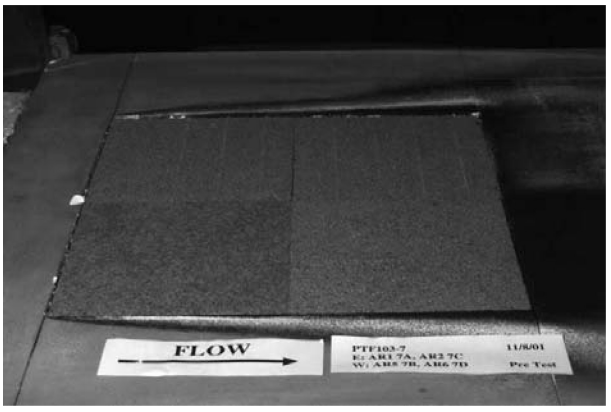

Fig. 10b Posttest photo of ARA Hyperlite materials from test at 5 W/cm^2.

Fig. 10c Posttest photo of ARA Hyperlite materials from test at 17 W/cm^2.

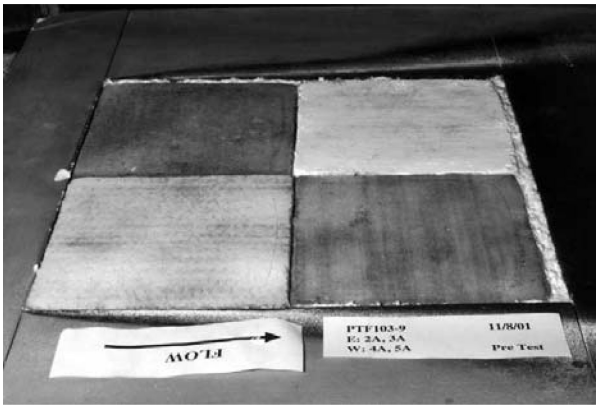

Fig. 11a Pretest photo of NASA flexible aerogel composite.

Fig. 11b Posttest photo of NASA flexible aerogel composite from test at 5 W/cm^2.

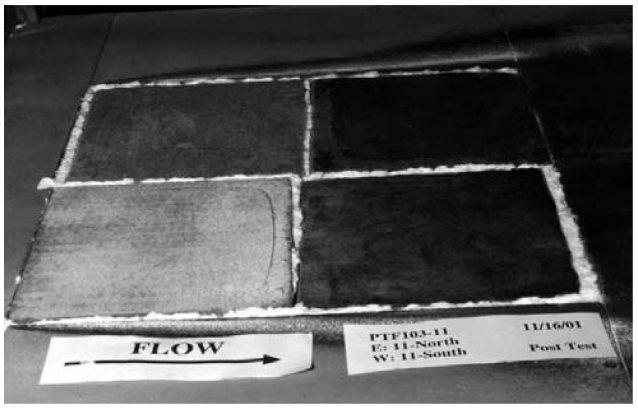

Fig. 11c Posttest photo of NASA flexible aerogel composite from test at 17 W/cm^2.

edges of the low heat-flux models because the flexibles were not as accurately sized to fill the test area as the other test materials. The flexibles' thermal performance was excellent, giving the lowest bondline temperatures of all screened materials.

Summary

A variety of candidate ablative materials for the Mars Science Laboratory TPS was evaluated in arcjet screening tests. Materials were tested at anticipated nominal and worst-case conditions for both forebody and backshell TPS applications. Several promising materials were identified, whereas others did not perform to expectations, particularly at the worst-case conditions. The best performing materials offer potential benefits in terms of performance, cost, and/or ease of manufacture and warrant further study. Because the MSL mission has been slipped to a 2009 launch, there is adequate time to optimize the TPS design for MSL.

Acknowledgments

This work would not have been possible without the assistance of numerous people at the Jet Propulsion Laboratory and NASA Ames Research Center. In particular, the authors acknowledge the efforts of Gary Allen of Eloret for the SLA-561V sizing analyses and the arcjet team from the Thermo-Physics Facilities Branch at NASA Ames Research Center for their efforts in conducting these well-executed test series.

References

[1]Brauer, G. L., Cornick, D. E., and Stevenson, R., "Capabilities and Applications of the Program to Optimize Simulated Trajectories (POST)," NASA CR-2770, Feb. 1977.

[2]Gnoffo, P. A., "An Upwind Based Point Implicit Relaxation Algorithm for Viscous Compressible Perfect Gas Flows," NASA TP 2953, Feb. 1990.

[3]Cheatwood, F. M., and Thompson, R. A., "The Addition of Algebraic Turbulence Modeling to Program LAURA," NASA TM 107758, April 1993.

[4]Cheatwood, F. M., and Gnoffo, P. A., "User's Manual for the Langley Aerothermodynamic Upwind Relaxation Algorithm (LAURA)," NASA TM-4674, April 1996.

[5]Congdon, W., and Curry, D., "Thermal Performance of Advanced Charring Ablator Systems for Future Robotic and Manned Missions to Mars," AIAA Paper 2001-2829, June 2001.

[6]Congdon, W., Curry, D., and Rarick, D., "Validation Arc-Jet Testing and Thermal-Response Modeling of Advanced Charring-Ablator Families," AIAA Paper 2002-2999, June 2002.

[7]Tran, H., Johnson, C., Rasky, D., and Hui, F., "Silicone Impregnated Reusable Ceramic Ablators for Mars Follow-On Missions," AIAA Paper 96-1819, June 1996.

[8]Hsu, M. S., and Chen, T. S., "Light-Weight Ceramic Insulation," U.S. Patent No. 6,339,034, issued 2002.

[9]Heister, N. K., and Clark, C. F., "Comparative Evaluation of Ablating Materials in Arc Plasma Jets," NASA CR-1207, Dec. 1968.

M. K. Lockwood
Guest Editor